

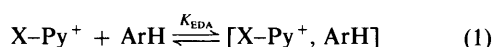
## Charge-transfer Structures of Aromatic EDA Complexes with *N*-Heteroatom-substituted Pyridinium Cations

Kwanyoung Y. Lee and Jay K. Kochi

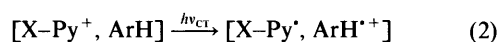
Chemistry Department, University of Houston, Houston, Texas 77204-5641, USA

*X*-Pyridinium cations with *N*-heteroatomic substituents such as *X* = halogen, nitro, alkoxy and acyloxy (*i.e.*,  $X\text{-NC}_5\text{H}_5^+$ ), in common with the ubiquitous *N*-alkylpyridinium cations, interact spontaneously with different benzene, naphthalene and anthracene donors (ArH) to afford a series of 1:1 charge-transfer complexes showing characteristic absorption spectra in the visible region. Quantitative evaluation of the electron-acceptor properties of  $X\text{-Py}^+$  (*via* an electrochemical reduction potential  $E_p^\circ$ ) indicates that the *N*-nitropyridinium ( $E_p^\circ = +0.10$  V), *N*-fluoropyridinium ( $E_p^\circ = -0.66$  V), *N*-acetoxypyridinium ( $E_p^\circ = -0.81$  V), and *N*-methoxypyridinium ( $E_p^\circ = -1.02$  V) cations are strong electrophiles in their charge-transfer interaction with aromatic donors to produce cofacial acceptor-donor pairs [ $X\text{-Py}^+$ , ArH] that are structurally related to the more common *N*-methylpyridinium ( $E_p^\circ = -1.32$  V) analogues.

A useful synthetic strategy in the activation of heteroaromatic nitrogen compounds such as pyridine, quinoline, *etc.* is prior conversion into a cationic *N*-substituted (pyridinium) derivative.<sup>1-4</sup> Such a transformation effectively converts a  $\pi$ -excessive aromatic compound into a  $\pi$ -deficient intermediate<sup>5</sup> that is significantly more reactive, particularly to nucleophilic attack.<sup>6-10</sup> The latter, in a more general context, considers *N*-alkylpyridinium electrophiles<sup>11</sup> as electron acceptors in intermolecular charge-transfer interactions.<sup>12-15</sup> Since a wide variety of other reactive *N*-*X*-substituted pyridinium cations are known with the electronegative substituent *X* = halogen (F, Cl, Br, I),<sup>16</sup> alkoxy,<sup>17</sup> acyloxy,<sup>18</sup> nitro,<sup>19</sup> *etc.*, it is desirable to compare these heteroatom-substituted pyridinium cations to the ubiquitous *N*-alkylpyridinium electrophiles. Toward this end, the charge-transfer interactions of the *N*-*X*-substituted pyridinium cations ( $X\text{-Py}^+$ ) may be exploited in the formation of electron donor-acceptor or EDA complexes with a graded series of common aromatic donors (ArH), as in eqn. (1) where



ArH includes various methylated benzenes, naphthalenes and anthracenes.<sup>20</sup> Particularly diagnostic of the formation of the EDA complexes in eqn. (1) are the characteristic new absorption bands that result from the intermolecular charge-transfer excitation ( $h\nu_{\text{CT}}$ ) according to Mulliken [eqn. (2)].<sup>21,22</sup> Indeed,



for a series of structurally related *N*-alkylpyridinium cations, the energies of the charge-transfer bands ( $h\nu_{\text{CT}}$ ) are known to be linearly correlated with the LUMO energies of the electron acceptor when *X* = methyl.<sup>23</sup>

The charge-transfer formulation in eqns. (1) and (2) represents the mechanistic basis for quantitatively interrelating the electrophilic properties of the *N*-alkylpyridinium cations with the wide array of heteroatom-substituted analogues. As such, we wish to establish in this study the charge-transfer structures that are available for the various aromatic EDA complexes derived from different types of pyridinium acceptors in eqn. (1). Most importantly, the electron-deficient (LUMO) character of each  $X\text{-Py}^+$ , as evaluated from the magnitude of the electrochemical reduction potential,<sup>24</sup> provides a quantitative guide for assessing the substituent (*X*) effect on charge-transfer

energies that are pertinent to electrophile-nucleophile interactions.<sup>25</sup> In the following report,<sup>26</sup> the charge-transfer excitation of  $X\text{-Py}^+$  and ArH is examined directly by time-resolved spectroscopy, and the fate of the reactive intermediates [ $X\text{Py}^\bullet$  and  $\text{ArH}^{\bullet+}$  in eqn. (2)] is traced to the various aromatic products resulting from the variation of the substituent *X*.

### Results

Each of the *N*-*X*-substituted pyridinium cations used in this study was prepared as a pure crystalline salt with the aid of Schlenk techniques. The hygroscopic sensitivity of the  $X\text{-Py}^+$  salts necessitated all subsequent handling to be carried out carefully with protection from atmospheric moisture (dry box). For example, *N*-fluoropyridinium and the 3,5-dichloro analogue were both isolated as the trifluoromethanesulfonate (triflate) salt by treating pyridine and 3,5-dichloropyridine, respectively, with fluorine in the presence of sodium triflate.<sup>27</sup> *N*-Acetoxypyridinium perchlorate and the 4-cyano derivative were prepared from pyridine and 4-cyanopyridine *N*-oxides by acetylation with a mixture of acetic anhydride and perchloric acid.<sup>28</sup> Analogously, these *N*-oxides were converted to crystalline *N*-methoxypyridinium and 4-cyano-*N*-methoxypyridinium salts by direct methylation with trimethyloxonium tetrafluoroborate.<sup>29</sup> The pyridinium salts with *N*-substituents of *X* = fluoro, acetoxy and methoxy thus join those with *X* = methyl<sup>30</sup> and nitro<sup>31</sup> to encompass a wide range of structurally similar heteroaromatic electrophiles for charge-transfer study in the following manner.

*Charge-transfer Spectra of X-Pyridinium Acceptors with Aromatic Donors.*—When a colourless solution of *N*-fluoropyridinium triflate in acetonitrile was treated with 9-methylanthracene, it immediately turned orange. Similarly, the addition of naphthalene led spontaneously to a bright yellow solution. The quantitative effects of such colour changes were apparent in the electronic (UV-VIS) spectra from the appearance of new absorptions in the visible region above 400 nm. Since these additional bands were incompletely resolved from the low-energy tail absorption of the cationic acceptor, *N*-fluoropyridinium was replaced by its 3,5-dichloro analogue to afford a red solution (with methylanthracene), in which the bathochromic shift of the new absorption was sufficient to reveal a well-resolved band at  $\lambda_{\text{max}} = 448$  nm. Fig. 1(a) also

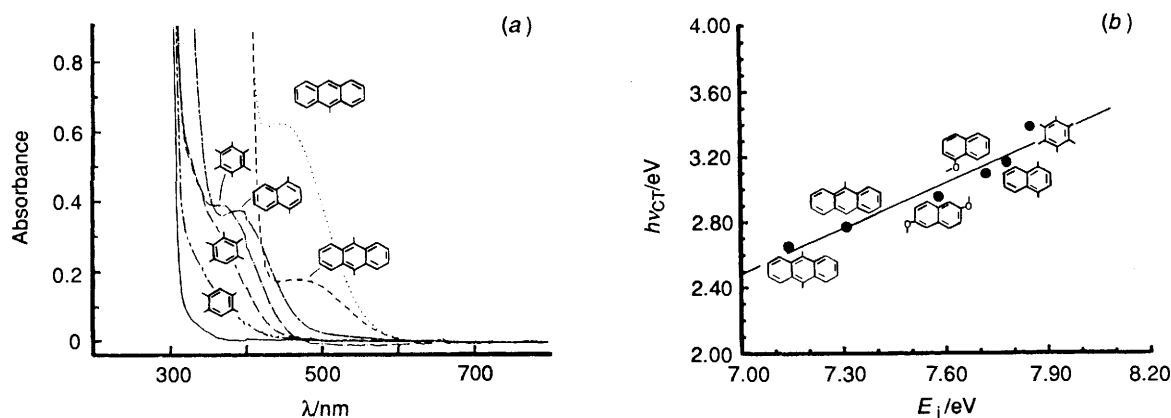


**Fig. 1** (a) Charge-transfer spectra of EDA complexes from  $0.03 \text{ mol dm}^{-3}$  3,5-dichloro-*N*-fluoropyridinium and various aromatic donors ( $0.03 \text{ mol dm}^{-3}$ , as indicated) in acetonitrile at  $0^\circ\text{C}$ , together with the low-energy tail of the acceptor alone (—). (b) Mulliken correlation of the charge-transfer transition energy ( $h\nu_{\text{CT}}$ ) with the ionization potential of the aromatic donors.

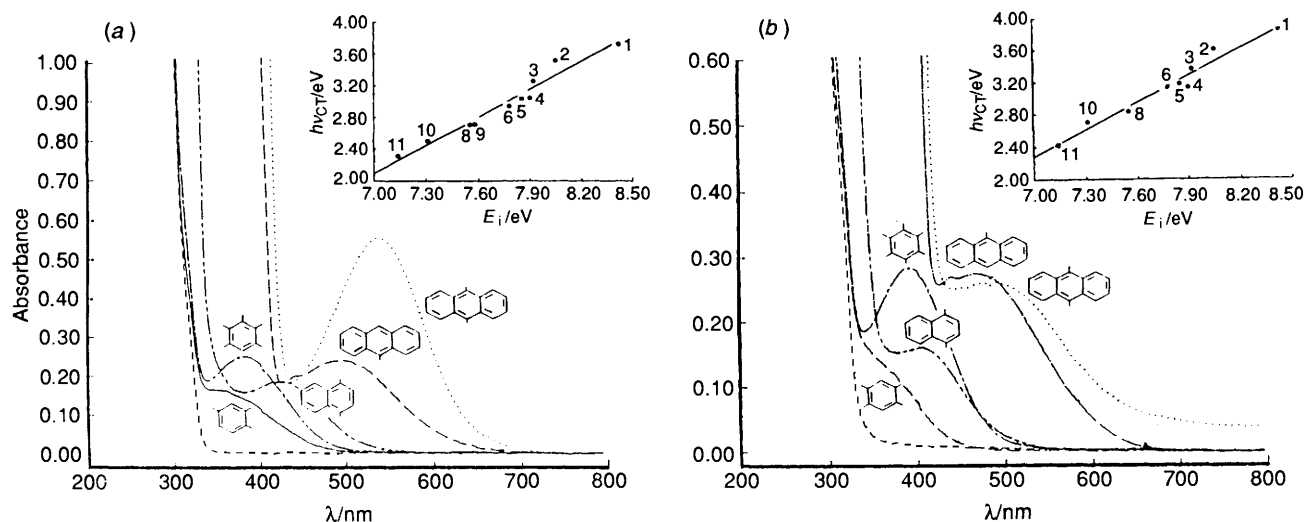


**Fig. 2** Comparative charge-transfer spectra from the various arenes (numbered as in Table 1) and (a) *N*-acetoxy-4-cyanopyridinium or (b) *N*-methoxy-4-cyanopyridinium acceptors in acetonitrile, showing the Mulliken correlations of  $h\nu_{\text{CT}}$  and  $E_i$  in the insets.

**Table 1** Charge-transfer spectra of aromatic EDA complexes with X-pyridinium cations<sup>a</sup>

Aromatic donor (ArH)	$E_i^b/\text{eV}$	X-Pyridinium acceptor, $h\nu_{\text{CT}}/\text{nm}^c$				
		AcO-Py(CN) <sup>+</sup>	MeO-Py(CN) <sup>+</sup>	F-Py(Cl <sub>2</sub> ) <sup>+</sup>	Me-Py(CN) <sup>+</sup>	O <sub>2</sub> N-Py <sup>+</sup> <sup>d</sup>
Mesitylene (1)	8.42	330	320	<i>e</i>	<i>e</i>	340
Durene (2)	8.05	354	345	<i>e</i>	330	352
Pentamethylbenzene (3)	7.92	382	369	<i>e</i>	354	389
1,4-Dimethoxybenzene (4)	7.90	408	397	<i>e</i>	—	—
Hexamethylbenzene (5)	7.85	410	392	367	378	408
1,4-Dimethylnaphthalene (6)	7.78	422	396	393	391	414
1-Methoxynaphthalene (7)	7.72	—	—	402	—	—
Anthracene (8)	7.55	460	438	<i>e</i>	—	—
2,6-Dimethoxynaphthalene (9)	7.58	458	—	421	—	—
9-Methylanthracene (10)	7.31	496	460	448	438	498
9,10-Dimethylanthracene (11)	7.14	537	512	468	—	526

<sup>a</sup> In acetonitrile solution at  $0^\circ\text{C}$ . <sup>b</sup> Ionization potential from ref. 32. <sup>c</sup> Py(CN) = 4-cyanopyridine, Py(Cl<sub>2</sub>) = 3,5-dichloropyridine. <sup>d</sup> From ref. 35. <sup>e</sup>  $\lambda_{\text{max}}(\text{CT})$  obscured by the local bands.

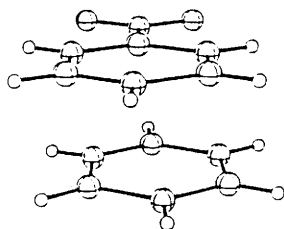
presents the family of new absorption bands obtained from 3,5-dichloro-*N*-fluoropyridinium and other aromatic donors such as mesitylene, durene, pentamethylbenzene, hexamethylbenzene, dimethylnaphthalene and dimethylanthracene. The progressive red shift with decreasing values of the ionization potentials ( $E_i$ ) of the aromatic donors,<sup>32</sup> as illustrated in Fig. 1(b), accords with the spectral assignment of the new bands to charge-transfer transitions.<sup>33</sup>

The addition of the same aromatic donors to X-pyridinium salts with X = acetoxy and methoxy caused similar colourations of the acetonitrile solutions, as shown in Fig. 2. The linear correlation of the charge-transfer bands ( $h\nu_{\text{CT}}$ ) with the ionization potentials of the arenes, as shown in the inset of each Figure, establishes the generality of the Mulliken prediction<sup>22</sup> as applied to these X-pyridinium cations.<sup>34</sup> Table 1 includes the pertinent charge-transfer energies of all the aromatic EDA

**Table 2** Formation constants of the EDA complexes of 1,4-dimethylnaphthalene with various X-pyridinium cations<sup>a</sup>

X-Py <sup>+</sup>	$\lambda_{\text{mon}}^b/$ nm	$K_{\text{EDA}}/$ dm <sup>-3</sup> mol <sup>-1</sup>	$\epsilon_{\text{CT}}/\text{dm}^3$ mol <sup>-1</sup> cm <sup>-1</sup>
4-Cyano- <i>N</i> -methoxypyridinium	406	0.76	310
4-Cyano- <i>N</i> -acetoxypyridinium	416	0.97	230
4-Cyano- <i>N</i> -methylpyridinium	410	0.33	680
<i>N</i> -Nitropyridinium <sup>c</sup>	450	1.1	210
3,5-Dichloro- <i>N</i> -fluoropyridinium	390	1.2	320

<sup>a</sup> In acetonitrile solutions containing 0.02–0.30 mol dm<sup>-3</sup> 1,4-dimethylnaphthalene and 0.02 mol dm<sup>-3</sup> X-pyridinium salt at 0 °C. <sup>b</sup> Monitoring wavelength. <sup>c</sup> From S. Sankararaman and J. K. Kochi, *J. Chem. Soc., Perkin Trans. 2*, 1991, 1. See also ref. 20.

**Fig. 3** Cofacial structure of the acceptor–donor pair

complexes with X-pyridinium cations including those with X = methyl as well as X = nitro available from the previous study.<sup>35</sup> Only the X-pyridinium–arene combinations that afforded resolved charge-transfer bands are included in Table 1, the exception being the mesitylene entries in which  $\lambda_{\text{max}}$  was obtained by digital subtraction of the component spectra from the CT (spectral) envelope.

**Formation Constants of the Aromatic EDA Complexes with X-Pyridinium Acceptors.**—The thermodynamic stabilities of the aromatic EDA complexes with various X-pyridinium acceptors were ascertained by measuring the formation constants  $K_{\text{EDA}}$  in eqn. (1) by the spectrophotometric procedure of Benesi and Hildebrand.<sup>36</sup> Owing to the solubility of all the X-pyridinium salts in acetonitrile, the charge-transfer absorbance  $A_{\text{CT}}$  was uniformly measured with 1,4-dimethylnaphthalene as the common arene donor (ArH) in excess. Under these conditions, the concentration dependence of  $A_{\text{CT}}$  is given by eqn. (3).<sup>37</sup> The

$$\frac{[\text{X-Py}^+]}{A_{\text{CT}}} = \frac{1}{K_{\text{CT}}\epsilon_{\text{CT}}[\text{ArH}]} + \frac{1}{\epsilon_{\text{CT}}} \quad (3)$$

linear fit of the absorbance data was obtained by the method of least squares, typically with a correlation coefficient of  $r > 0.99$ , and the resulting values of the formation constant  $K_{\text{EDA}}$  and the extinction coefficient  $\epsilon_{\text{CT}}$  (at the monitoring wavelength), extracted from the slope and intercept, respectively, are listed in Table 2.

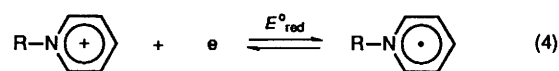
The relatively invariant values of  $K_{\text{EDA}}$  and  $\epsilon_{\text{CT}}$ , as evaluated for the various EDA complexes [X-Py<sup>+</sup>, ArH], indicate that the stabilities and donor–acceptor interactions were completely independent of the substituent change from X = fluoro, methoxy, acetoxy, nitro and methyl. Accordingly, we infer that the X-pyridinium acceptors are not differentiated insofar as the charge-transfer structures of the aromatic EDA complexes are concerned.

**Isolation of Crystalline EDA Complexes of Aromatic Donors with X-Pyridinium Acceptors.**—Despite the limited magnitudes of the formation constants in Table 2, our previous successful isolation of similarly weak EDA complexes,<sup>34</sup> encouraged us to

grow single crystals of [X-Py<sup>+</sup>, ArH] for X-ray crystallographic analysis.

Various attempts to crystallize the aromatic EDA complexes with different *N*-nitropyridinium acceptors usually led to the prior separation of the (colourless) ionic salt without the aromatic donor. However, by employing the evaporative technique found to be effective with another salt/neutral combination,<sup>34a</sup> we were finally able to isolate yellow microcrystals of the EDA complexes of 1-methylnaphthalene and 1,4-dimethylnaphthalene with 4-methoxy-*N*-nitropyridinium tetrafluoroborate, with the 1:1 stoichiometric composition determined by NMR analysis.<sup>35</sup> Unfortunately, repeated attempts did not yield single crystals suitable for X-ray crystallography. Similarly unsuccessful were attempts to crystallize different aromatic EDA complexes with *N*-acetoxy-4-cyanopyridinium perchlorate, and crystallization generally led to the separation of either the pure pyridinium acceptor or the arene donor. Of the other X-pyridinium salts, only the *N*-methoxy derivative of 4-cyanopyridine deposited pale yellow crystals of the 1:1 complex with durene and 1,4-dimethylnaphthalene, but these were also unsuitable for X-ray crystallography. However, the charge-transfer structure relevant to the aromatic EDA complexes with X-pyridinium could be deduced from the X-ray crystal structure of the related bis(*N*-methylpyridinium) acceptor which was determined previously.<sup>38</sup> Together with the strong correlation of the CT spectral properties, with those of the aromatic EDA complexes with the (cationic) tropylium acceptor,<sup>34a</sup> we conclude that the cofacial structure of the acceptor–donor pair also applies to [X-Py<sup>+</sup>, ArH], as graphically illustrated in Fig. 3 (X = NO<sub>2</sub>).<sup>35</sup>

**Electrochemical Evaluation of X-Pyridinium Cations as Electron Acceptors.**—The acceptor (LUMO) properties of *N*-alkylpyridinium cations are related to the reversible potential  $E_{\text{red}}^{\circ}$  for the one-electron reduction to the *N*-alkylpyridinyl radical, [eqn. (4)].<sup>39</sup>



The cyclic voltammogram of the 4-cyano derivative of the *N*-methylpyridinium cation exhibited a well-defined one-electron cathodic wave at  $E_{\text{p}}^{\text{c}} = -0.67$  V on the initial negative scan, and the coupled anodic wave at  $E_{\text{p}}^{\text{a}} = -0.60$  V on the return scan at  $v = 0.5$  V s<sup>-1</sup> in acetonitrile containing 0.1 mol dm<sup>-3</sup> tetrabutylammonium hexafluorophosphate (TBAH) as the supporting electrolyte. Chemical reversibility of the redox equilibrium, as indicated by the anodic/cathodic peak current ratio  $i_{\text{p}}^{\text{a}}/i_{\text{p}}^{\text{c}}$  of unity in Fig. 4, was achieved even at the relatively slow scan rate of  $v = 0.01$  V s<sup>-1</sup>. This is undoubtedly due to the stability (persistence) of the 4-cyano-*N*-methylpyridinyl radical.<sup>40</sup> The standard reduction potential for this redox couple was evaluated as  $E_{\text{red}}^{\circ} = -0.64$  V vs. SCE from the constant value of  $(E_{\text{p}}^{\text{c}} + E_{\text{p}}^{\text{a}})/2$  at various scan rates.<sup>41</sup> Moreover, the cathodic/anodic peak separation ( $E_{\text{p}}^{\text{c}} - E_{\text{p}}^{\text{a}}$ ) close to 60 mV, which showed little variation with sweep rate ( $\sim 10$  mV/log  $v$ ) with sweep rates up to 1.0 V s<sup>-1</sup>, indicated an electrochemically reversible electron transfer [eqn. (4)].

By comparison, the cyclic voltammogram of the parent *N*-methylpyridinium cation showed the cathodic wave at the significantly (negative) shifted potential of  $E_{\text{p}}^{\text{c}} = -1.32$  V at the same scan rate. More revealingly, the absence of the coupled anodic wave on the return scan, even at sweep rates as high as 100 000 V s<sup>-1</sup>, indicated that the one-electron reduction of the methylpyridinium cation in eqn. (4) was chemically irreversible owing to the fast (encounter-controlled) dimerization of the reactive *N*-methylpyridinyl radical.<sup>42</sup>

**Table 3** Reduction potentials of X-pyridinium cations<sup>a</sup>

X	X-Py(Y) Y	$E_p^c/V$ vs. SCE	$\lambda_{\max}(\text{CT})^c/$ nm
CH <sub>3</sub>	H	-1.32	~290
	4-CN	-0.67 <sup>d</sup>	378
OCH <sub>3</sub>	H	-1.02	308
	4-CN	-0.30	392
OCOCH <sub>3</sub>	H	-0.81	310
	4-CN	0.10	410
F	H	-0.66	320
	3,5-Cl <sub>2</sub>	-0.40	367
H	H	-0.65 <sup>e</sup>	~300
	NO <sub>2</sub> <sup>f</sup>	4-OCH <sub>3</sub>	-0.10
NO <sub>2</sub> <sup>f</sup>	4-CH <sub>3</sub>	0.06	408
	H	0.10	422
	4-Cl	0.25	436 <sup>g</sup>
	4-OCOCH <sub>3</sub>	0.31	462 <sup>g</sup>
	4-CN	0.50	—

<sup>a</sup> From the initial negative-scan cyclic voltammogram in acetonitrile containing 0.1 mol dm<sup>-3</sup> TBAH at  $v = 0.5 \text{ V s}^{-1}$  and 23 °C. <sup>b</sup> Cathodic peak potential, unless indicated otherwise. <sup>c</sup> Charge-transfer band from hexamethylbenzene complex in acetonitrile at 0 °C, unless indicated otherwise. <sup>d</sup> Cathodic peak potential of reversible cyclic voltammogram. <sup>e</sup> Partially reversible. <sup>f</sup> From ref. 35. <sup>g</sup> At -40 °C.

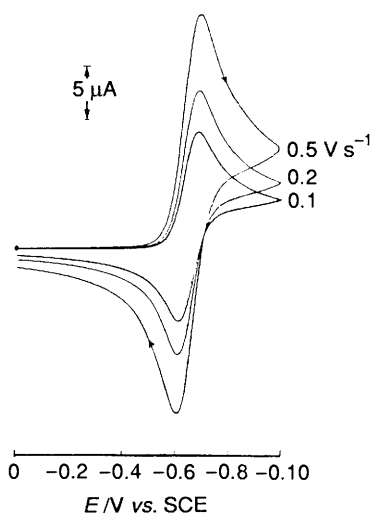


**Fig. 4** The initial negative-scan cyclic voltammogram of 4-cyano-*N*-methylpyridinium (5 mmol dm<sup>-3</sup>) in acetonitrile containing 0.1 mol dm<sup>-3</sup> TBAH at the scan rates indicated

The reductive behaviour of X-pyridinium cations with the heteroatom substituents X = methoxy, acetoxy and fluoro was similar to that of *N*-methylpyridinium in that the initial negative-scan cyclic voltammogram consistently showed a single cathodic wave, but no coupled anodic wave was visible on the return scan. However, unlike the *N*-methylpyridinium acceptor, the presence of a 4-cyano substituent on the *N*-methoxy, the *N*-acetoxy or the *N*-fluoro-pyridinium cation did not confer sufficient (kinetic) stability on the X-pyridinyl radical for us to observe reversible cyclic voltammetric behaviour, even at scan rates exceeding  $v = 50\,000 \text{ V s}^{-1}$ .

The cathodic peak potentials  $E_p^c$  of the various X-pyridinium cations measured under standard conditions ( $v = 0.5 \text{ V s}^{-1}$  in acetonitrile containing 0.1 mol dm<sup>-3</sup> TBAH at 23 °C) are collected in Table 3, together with those for X = nitro.<sup>35</sup> Table 3 (column 4) also lists the charge-transfer energies ( $h\nu_{\text{CT}}$ ) of the corresponding EDA complexes formed from a common aromatic donor (hexamethylbenzene) in acetonitrile.

The direct relationship between the (irreversible) reduction potential ( $E_p^c$ ) of the X-pyridinium cation and the charge-

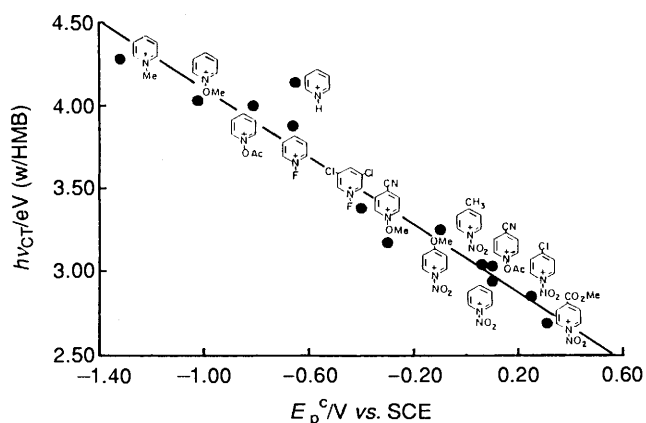


**Fig. 5** Spectral shifts of the charge-transfer bands ( $h\nu_{\text{CT}}$ ) of hexamethylbenzene EDA complexes with the variation in the reduction potentials ( $E_p^c$ ) of the various X-pyridinium acceptors indicated

transfer energy ( $h\nu_{\text{CT}}$ ) of the EDA complex is illustrated in Fig. 5. The line represents the least-squares slope analytically expressed (in volts) as in eqn. (5) with a correlation coefficient of

$$E_p^c = 1.0h\nu_{\text{CT}} + 3.0 \quad (5)$$

$r = 0.97$ . Although the latter represents some scatter of the experimental points, the unmistakable correlation of all the X-pyridinium cations (including X = hydrogen) indicates that the charge-transfer characteristics of the X-pyridinium acceptors arise largely from the electronegative substituent X, more or less independently of steric factors.

## Discussion

The various *N*-substituted pyridinium cations (X-Py<sup>+</sup>) with the substituent X = nitro, methoxy, fluoro, acetoxy and methyl are excellent electron acceptors by virtue of the wide range of charge-transfer interactions that are induced with different aromatic donors, as shown by the family of characteristic intermolecular absorption bands in Figs. 1(a) and 2. The linear correlations of the charge-transfer energies ( $h\nu_{\text{CT}}$ ) with the ionization potentials of the aromatic donors, presented in Figs. 1(b) and 2 (insets) for each X-pyridinium acceptor, accord with the predictions of Mulliken theory generally expressed as eqn. (6).<sup>22,33</sup> The energy gap ( $E_i - \text{EA}$ ) represents the HOMO-

$$h\nu_{\text{CT}} = E_i - \text{EA} + \omega \quad (6)$$

LUMO separation of the aromatic donor and the X-pyridinium acceptor in the EDA complex.<sup>43</sup> Since the electron affinity (EA) and the interaction term ( $\omega$ ) in eqn. (6) are constant for a given X-pyridinium acceptor, the direct relationship between  $h\nu_{\text{CT}}$  and  $E_i$  establishes the charge-transfer character of the absorption changes in Figs. 1 and 2.<sup>33</sup>

The Mulliken relationship in eqn. (6) also predicts a linear correlation of the charge-transfer energy with the electron affinity (EA) for a series of EDA complexes derived from a single aromatic donor with various X-pyridinium cations. Thus the striking correlation shown in Fig. 5 for the hexamethylbenzene EDA complexes indicates that the electrochemical reduction potential  $E_p^c$  provides a useful measure of the electron affinity of a cationic acceptor, such as the X-pyridinium cations, which is otherwise difficult to measure experimentally.<sup>44</sup> The general applicability of  $E_p^c$  in this capacity is emphasized by the linear relationship in Fig. 6, which represents the global effect of all the charge-transfer interactions. It encompasses every combination of the different X-pyridinium acceptors and the graded

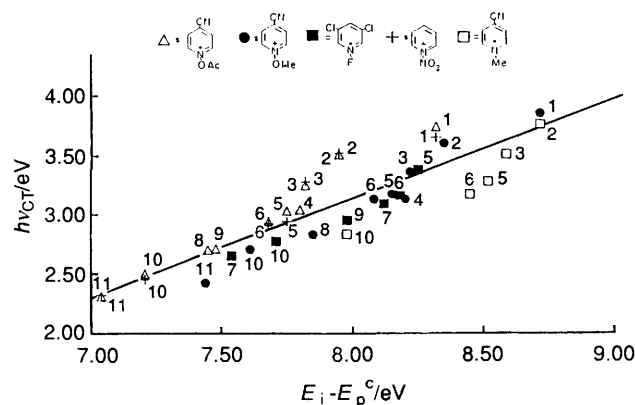


Fig. 6 Generalized Mulliken correlation of charge-transfer transition energies ( $h\nu_{CT}$ ) with the HOMO-LUMO gap for the various EDA complexes from the X-pyridinium acceptors (shown at the top) and the aromatic donors (numbered) in Table 1.

series of aromatic donors listed in Table 1 within a single Mulliken correlation [eqn. (7)] that is expressed in volts

$$h\nu_{CT} = E_i - E_p^c - 3.0 \quad (7)$$

( $r = 0.93$ ). The linear correlation spans the HOMO-LUMO gap of almost  $50 \text{ kcal mol}^{-1}$ ,\* and includes diverse pyridinium cations containing strongly differentiated heteroatom substituents (such as X = nitro, fluoro, acetoxy) together with the more conventional *N*-alkylpyridinium cations (X = methyl).

The slope of unity in Fig. 6 reflects the formation of uniformly weak EDA complexes,<sup>21,43</sup> and it is supported by the spectrophotometric measurements of the formation constants  $K_{EDA}$  in Table 2. For the EDA complexes in general, the binding of the electron donor (D) to the electron acceptor (A) is generally described in valence-bond terms by eqn. (8)<sup>43</sup> where the ground-

$$\psi_{GS} = \frac{1}{N} [a\varphi_0 + b\varphi_1 + \dots] \quad (8)$$

state wave function  $\psi_{GS}$  mainly contains contributions from  $\varphi_0$  and  $\varphi_1$  representing weak van der Waals or the no-bond interaction of D and A and the dative or charge-transfer component  $D^+ A^-$ , respectively, and  $N$  is the normalization factor. The formation constants of such weak EDA complexes as  $[X\text{-Py}^+, \text{ArH}]$  show no dependence on the electron affinity of the X-pyridinium acceptor (see Table 2), and the charge-transfer contribution is minor, *i.e.*  $a^2 \gg b^2$ . It is thus likely that the cofacial structure shown in Fig. 3 is equally applicable to all X-pyridinium EDA complexes, irrespective of the acceptor strength. According to Mulliken theory, the imbalance also qualitatively applies to the charge-transfer excited state [eqn. (9)], in which the charge-transfer contribution dominates, *i.e.*

$$\psi_{ES} = \frac{1}{N'} [b\varphi_0 - a\varphi_1 + \dots] \quad (9)$$

$b^2 \ll a^2$ ,<sup>21</sup> as depicted in eqn. (2). Under these circumstances, the acceptor contribution corresponds to the (complete) transformation of the X-pyridinium cation to the X-pyridinyl radical, the energy requirement for which is given by the value of  $E_{red}^0$  in eqn. (4). The cyclic voltammetric determination of  $E_{red}^0$  from the reversible redox change (such as 4-cyano-*N*-methylpyridinium in Fig. 3) can be applied to chemically irreversible systems such as the X-pyridinium cations with X = nitro, methoxy, fluoro and acetoxy if the lifetimes of the X-pyridinyl radical are

short relative to the electrochemical timescale.<sup>45</sup> Under these circumstances, the cyclic voltammetric peak potential  $E_p^c$  is directly related to  $E_{red}^0$ .<sup>46</sup> In the case of the *N*-nitropyridinium cations, the short lifetimes have been shown to arise from the facile homolysis of the *N*-nitropyridinyl radical [eqn. (10)].<sup>35</sup>



Other studies indicate that the *N*-fluoropyridinyl and *N*-alkoxy-pyridinyl radicals are similarly prone to undergo rapid homolysis.<sup>47,48</sup> Time-resolved spectroscopy and photochemistry of aromatic EDA complexes with X-pyridinium cations, to be described in the following study,<sup>26</sup> will further amplify the integral role that the homolytic scission of X-pyridinyl radicals plays in charge-transfer activation.

## Experimental

**Materials.**—Durene (Aldrich), pentamethylbenzene (Aldrich), hexamethylbenzene (Aldrich) and 9-methylanthracene (Aldrich) were recrystallized from absolute ethanol, and naphthalene (Aldrich) was sublimed *in vacuo*. 1,4-Dimethylnaphthalene (Aldrich), 9,10-dimethylnaphthalene (Aldrich), 2,6-dimethoxynaphthalene (Aldrich) were used as received. Acetonitrile (Fisher) was stirred with  $\text{KMnO}_4$  for 24 h, and the mixture refluxed until the liquid was colourless. After removal of the brown  $\text{MnO}_2$  filtration, the acetonitrile was distilled from  $\text{P}_2\text{O}_5$  under an argon atmosphere. Pyridine (Aldrich) was distilled from solid KOH, and pyridine *N*-oxide (Aldrich) was sublimed *in vacuo*. 3,5-Dichloropyridine and 4-cyanopyridine *N*-oxide were used as received. All analyses were carried out by Atlantic Microlab, Atlanta, GA.

Crystalline *N*-fluoropyridinium salts ( $X\text{-Py}^+ \text{OTf}^-$ ) were prepared by treating the corresponding pyridine with fluorine (10%) diluted in nitrogen (Air Products) in the presence of either sodium triflate (Py) or lithium triflate (3,5- $\text{Cl}_2\text{Py}$ ) following the literature procedure.<sup>27</sup>  $\text{F-Py}^+ \text{OTf}^-$ :  $\delta_{\text{H}}(\text{CD}_3\text{CN})$  8.27 (2 H, t), 8.68 (1 H, t), 9.21 (2 H, dd).  $\delta_{\text{F}}$  -45.9 (s, 1 F), 80.2 (s, 3 F). 3,5-Dichloro-*N*-fluoropyridinium triflate:  $\delta_{\text{H}}(\text{CD}_3\text{CN})$  9.57 (2 H, dt,  $J$  14, 2), 8.83 (1 H, t,  $J$  2).  $\delta_{\text{F}}(\text{CD}_3\text{CN})$  -50.6 (s, 1 F), 80.7 (s, 3 F). *N*-Acetoxypyridinium perchlorate was prepared by treating pyridine *N*-oxide with 70% perchloric acid in acetic acid following the literature procedure.<sup>28</sup> The colourless precipitates were recrystallized from a mixture of acetonitrile and diethyl ether.  $\delta_{\text{H}}(\text{CD}_3\text{CN})$  2.50 (s, 3 H), 8.23 (2 H, t), 8.69 (1 H, t), 8.86 (2 H, d). *N*-Acetoxy-4-cyanopyridinium perchlorate: to a cold (0 °C) suspension of 4-cyanopyridine *N*-oxide (0.55 g) in acetic anhydride (20  $\text{cm}^3$ ) was slowly added 0.1 mol  $\text{dm}^{-3}$  perchloric acid in acetic acid (46  $\text{cm}^3$ ). After 20  $\text{cm}^3$  of  $\text{HClO}_4/\text{AcOH}$  mixture was added, the mixture became clear, and the further (30  $\text{cm}^3$ ) addition afforded colourless crystals which were collected by filtration and recrystallized from a mixture of  $\text{CH}_3\text{CN}$  and diethyl ether to yield very hygroscopic colourless crystals.  $\delta_{\text{H}}(\text{CD}_3\text{CN})$  2.52 (3 H, s), 8.46 (2 H, d,  $J$  7.6), 9.01 (2 H, d) [Found: C, 36.9; H, 2.8; N, 10.8. Calc. for  $\text{C}_8\text{H}_7\text{ClN}_2\text{O}_6$  (262.6): C, 36.59; H, 2.69; N, 10.67%]. Preparation of the *N*-methoxypyridinium salt was initially attempted by treating pyridine *N*-oxide with either methyl sulfate or methyl triflate following the literature procedures,<sup>9,29</sup> but the crystalline salt could not be obtained. The use of trimethyloxonium salt  $\text{Me}_3\text{O}^+ \text{BF}_4^-$  (Aldrich) afforded the crystalline  $\text{MeO-Py}^+ \text{BF}_4^-$  in the following manner. To a suspension of trimethyloxonium tetrafluoroborate (0.79 g) in dichloromethane (20  $\text{cm}^3$ ) was slowly added a solution of pyridine *N*-oxide (0.5 g). The salts gradually dissolved and the solution became turbid. After being stirred for 30 min, the solvent was

\* 1 cal = 4.184 J.

evaporated under-reduced pressure. The residue was recrystallized from a mixture of acetonitrile and diethyl ether.  $\delta_{\text{H}}(\text{CD}_3\text{CN})$  4.39 (3 H, s), 8.12 (2 H, t), 8.54 (1 H, t), 8.97 (2 H, d) [Found: C, 36.4; H, 4.1; N, 7.10. Calc. for  $\text{C}_6\text{H}_8\text{BF}_4\text{NO}$  (197.0): C, 36.59; H, 4.10; N, 7.11%]. 4-Cyano-*N*-methoxy-pyridinium tetrafluoroborate: the salt was prepared from 4-cyanopyridine *N*-oxide following the procedure above. Recrystallization from a mixture of acetonitrile and diethyl ether yielded hygroscopic white crystals.  $\delta_{\text{H}}(\text{CD}_3\text{CN})$  4.46 (3 H, s), 8.44 (2 H, d, *J* 7.4), 9.17 (2 H, d) (Found: C, 38.00; H, 3.2; N, 12.60. Calc. for  $\text{C}_7\text{H}_7\text{BF}_4\text{N}_2\text{O}$  (222.0): C, 37.87; H, 3.19; N, 12.62%).

**Instrumentation.**—The UV–VIS absorption spectra were measured on a Hewlett-Packard 8450A diode-array spectrometer equipped with a HP 89100A temperature controller. The  $^1\text{H}$  and  $^{19}\text{F}$  NMR spectra were recorded on a JEOL FX 90Q spectrometer operating at 90 MHz. The proton chemical shifts are reported in ppm from tetramethylsilane, and the  $^{19}\text{F}$  chemical shifts are reported in ppm upfield from a fluorotrichloromethane internal standard. *J* values are in Hz. Cyclic voltammetry was performed on an iR-compensated potentiostat driven by a Princeton Applied Research (PAR) 175 universal programmer. Current–voltage curves were plotted on a Houston Series 2000 X-Y recorder or displayed on a Gould Biomation (model 4500) digital oscilloscope. The working electrode consisted of a platinum disk ( $r = 0.5$  mm) embedded in glass, and a platinum gauze was used as a counter electrode.<sup>49</sup> Potentials were measured relative to a SCE reference electrode ( $E^\circ$  for  $\text{Cp}_2\text{Fe}/\text{Cp}_2\text{Fe}^+ = 0.41$  V). All *N*-fluoro, *N*-methoxy and *N*-acetoxypyridinium cations exhibited some degree of an adsorption (coating) problem.<sup>50</sup> Since the cyclic voltammograms showed non-faradaic currents after several scans, the Pt electrode was polished with alumina (1  $\mu$ ) on an emery cloth surface after every scan. The reproducibility of the values of  $E_p^c$  achieved in this manner was  $\pm 0.02$  V, except for *N*-fluoropyridinium and 3,5-dichloro-*N*-fluoropyridinium in which the error was estimated to be  $\pm 0.05$  V.

**Charge-transfer Spectral Measurements.**—Into a 10 mm quartz cuvette equipped with a side arm and a Schlenk adaptor,  $6 \times 10^{-5}$  mol of the appropriate X-pyridinium salt was typically added (dry box), and the cell was connected to a vacuum line. Acetonitrile (1  $\text{cm}^3$ ) was added with the aid of a hypodermic syringe and a 2  $\text{cm}^3$  aliquot of 0.04  $\text{mol dm}^{-3}$  aromatic donor in acetonitrile was carefully cannulated into the side arm of the UV cell. The cuvette was thermally equilibrated in an ice bath, and the solutions were mixed. The charge-transfer absorption spectra were measured at various concentrations of X-pyridinium salt (0.02–0.05  $\text{mol dm}^{-3}$ ) and an aromatic donor (0.01–0.1  $\text{mol dm}^{-3}$ ), to ensure that the band maxima were invariant. When  $\lambda_{\text{max}}$  was close to 300 nm (*i.e.* the tail of the hexamethylbenzene absorption), as with the *N*-fluoro, *N*-methoxy, *N*-acetoxy, *N*-methyl and hydropyridinium cations, the charge-transfer spectra were measured at low concentrations of hexamethylbenzene (5  $\text{mol dm}^{-3}$ ) and relatively high concentrations of the cationic acceptors (0.1  $\text{mol dm}^{-3}$ ).

**Spectrophotometric Determination of the Formation Constant.**—An aliquot of 0.02  $\text{mol dm}^{-3}$  3,5-dichloro-*N*-fluoropyridinium triflate in acetonitrile (3  $\text{cm}^3$ ) was placed in a UV cell. The cuvette was cooled in an ice bath, and 1,4-dimethylnaphthalene was added incrementally (0.06–0.9 mmol). The absorbance changes were measured at 390, 406, 420 nm, where both components individually did not absorb. From the plot of  $[\text{X-Py}^+]/A_{\text{CT}}$  vs.  $[\text{1,4-dimethylnaphthalene}]^{-1}$ , the slope was estimated as  $(\epsilon_{\text{CT}}K_{\text{CT}})^{-1}$  and the intercept as  $\epsilon_{\text{CT}}^{-1}$ . The formation constant  $K_{\text{CT}}$  was  $1.17 \pm 0.05 \text{ dm}^3 \text{ mol}^{-1}$  and  $\epsilon_{\text{CT}} =$

323 (390 nm), 293 (406 nm) and 268 (420 nm)  $\text{dm}^3 \text{ mol}^{-1} \text{ cm}^{-1}$ . Each of the linear fits obtained by the least squares method has a correlation coefficient of at least  $r > 0.99$ . The formation constant for *N*-acetoxy- and *N*-methoxy-4-cyanopyridinium cation with 1,4-dimethylnaphthalene was determined in a similar manner (Table 2).

### Acknowledgements

We thank the National Science Foundation, the R. A. Welch Foundation and the Texas Advanced Research Project for financial support.

### References

- O. R. Rodig, *Quaternary Pyridinium Compounds*, in *Pyridine and Its Derivatives*, ed. R. A. Abramovich, Suppl. Pt I, vol. 14, Wiley, New York, 1974, p. 309 ff.
- D. L. Comins and S. O'Connor, *Adv. Heterocyclic Chem.*, 1988, **44**, 200.
- E. Ochiai, *Aromatic Amine Oxides*, Elsevier, New York, 1967, ch. 7; A. R. Katritzky and J. M. Lagowski, *Chemistry of the Heterocyclic N-Oxides*, Academic, New York, 1971, p. 258 ff.
- S. Oae, T. Kitao and Y. Kitaoka, *J. Am. Chem. Soc.*, 1962, **84**, 3359, 3362; V. Boekelheide and W. J. Linn, *J. Am. Chem. Soc.*, 1954, **76**, 1286.
- R. A. Abramovitch and I. Shinkai, *Acc. Chem. Res.*, 1976, **9**, 192.
- L. Bauer and L. A. Gardella, *J. Org. Chem.*, 1963, **28**, 1323.
- O. Cervinka, *Collect. Czech. Chem. Commun.*, 1962, **27**, 567.
- R. Eisenthal and A. R. Katritzky, *Tetrahedron*, 1965, **21**, 2205.
- W. E. Feely and E. M. Beavers, *J. Am. Chem. Soc.*, 1959, **81**, 4004.
- E. Ochiai, *J. Org. Chem.*, 1953, **18**, 534; P. S. Mariano, *Acc. Chem. Res.*, 1983, **16**, 130.
- A. R. Katritzky and G. Masumarra, *Chem. Soc. Rev.*, 1984, **13**, 47.
- E. LeGoff and R. B. LaCount, *J. Am. Chem. Soc.*, 1963, **85**, 1354.
- T. G. Beaumont and K. M. C. Davis, *J. Chem. Soc. B*, 1968, 1010; T. G. Beaumont and K. M. C. Davis, *Nature (London)*, 1970, **225**, 632.
- S. F. Mason, *J. Chem. Soc.*, 1960, 2437; J. Nasielski and E. Vander Donck, *Theor. Chim. Acta*, 1964, **2**, 22.
- E. M. Kosower and J. A. Skorz, *J. Am. Chem. Soc.*, 1960, **82**, 2195.
- J. Barluenga, M. A. Rodriguez and P. J. Campos, *J. Org. Chem.*, 1990, **55**, 3104; G. B. Kauffman and K. L. Stevens, *Inorg. Synth.*, 1963, **7**, 169; T. Umemoto and K. Tomita, *Tetrahedron Lett.*, 1986, **27**, 3271. Compare also N. W. Alcock and G. B. Robertson, *J. Chem. Soc., Dalton Trans.*, 1975, 2483; O. Hassel and H. Hope, *Acta Chem. Scand.*, 1961, **15**, 407; I. Haque and J. L. Wood, *J. Mol. Struct.*, 1968, **2**, 217; M. Schmeisser, W. Fink and K. Brändle, *Angew. Chem.*, 1957, **67**, 780.
- W. E. Feely, W. L. Lehn and V. Boekelheide, *J. Org. Chem.*, 1957, **22**, 1135.
- C. W. Muth, R. S. Darlak, W. H. English and A. T. Hamner, *Anal. Chem.*, 1962, **34**, 1163.
- G. A. Olah, J. A. Olah and N. A. Overchuk, *J. Org. Chem.*, 1965, **30**, 3373; J. Jones and J. Jones, *Tetrahedron Lett.*, 1964, 2117.
- J. W. Verhoeven, I. P. Dirx and Th. J. De Boer, *Tetrahedron*, 1969, **25**, 3395. See also A. S. N. Murthy and A. P. Bhardwaj, *Spectrochim. Acta, Part A*, 1983, **39**, 939.
- R. S. Mulliken, *J. Am. Chem. Soc.*, 1950, **72**, 601.
- R. S. Mulliken and W. B. Person, *Molecular Complexes*, Wiley, New York, 1969.
- C. Párkányi and G. J. Leu, *Z. Naturforsch., Teil B*, 1975, **30**, 984.
- G. Briegleb, *Elektronen Donator Acceptor Komplexe*, Springer, Berlin, 1961.
- J. K. Kochi, *Angew. Chem., Int. Ed. Engl.*, 1988, **27**, 1227.
- T. M. Bockman, K. Y. Lee, J. K. Kochi, *J. Chem. Soc., Perkin Trans. 2*, 1992, in press (2/01806C).
- T. Umemoto, K. Tomita and K. Kawada, *Org. Synth.*, 1990, **69**, 129.
- C. W. Muth and R. S. Darlak, *J. Org. Chem.*, 1965, **30**, 1909.
- A. R. Katritzky, *J. Chem. Soc.*, 1956, 2404.
- E. M. Kosower and P. E. Klinedinst, Jr., *J. Am. Chem. Soc.*, 1956, **78**, 3493.
- G. A. Olah, S. C. Narang, J. A. Olah, R. L. Pearson and C. A. Cupas, *J. Am. Chem. Soc.*, 1980, **102**, 3507.
- (a) J. O. Howell, J. M. Goncalves, C. Amatore, L. Klasinc, R. M. Wightman and J. K. Kochi, *J. Am. Chem. Soc.*, 1984, **106**, 3968; (b) J. M. Masnovi, E. A. Seddon and J. K. Kochi, *Can. J. Chem.*, 1984,

- 62, 2552; (c) P. Nounou, *J. Chim. Phys.*, 1966, **63**, 994; (d) H. Bock, G. Wagner and J. Kroner, *Chem. Ber.*, 1972, **105**, 3850; (e) O. B. Nagy, S. Dupire and J. B. Nagy, *Tetrahedron*, 1975, **31**, 2453.
- 33 R. Foster, *Organic Charge-Transfer Complexes*, Academic, New York, 1969.
- 34 Compare (a) Y. Takahashi, S. Sankararaman and J. K. Kochi, *J. Am. Chem. Soc.*, 1989, **111**, 2954; (b) J. M. Wallis and J. K. Kochi, *J. Am. Chem. Soc.*, 1988, **110**, 8207.
- 35 E. K. Kim, K. Y. Lee and J. K. Kochi, *J. Am. Chem. Soc.*, 1992, **114**, 1756.
- 36 H. G. Benesi and J. H. Hildebrand, *J. Am. Chem. Soc.*, 1949, **71**, 2703.
- 37 W. B. Person, *J. Am. Chem. Soc.*, 1965, **87**, 167; R. Foster, *Molecular Complexes*, 1974, **2**, 107.
- 38 K. B. Yoon and J. K. Kochi, *J. Phys. Chem.*, 1991, **95**, 3780.
- 39 See: S. Hünig and W. Schenk, *Liebigs Ann. Chem.*, 1979, 1523; E. M. Kosower, D. Hofmann and K. Wallenfels, *J. Am. Chem. Soc.*, 1962, **84**, 2755; T. M. Bockman and J. K. Kochi, *J. Am. Chem. Soc.*, 1989, **111**, 4669.
- 40 M. Itoh and S. Nagakura, *Bull. Chem. Soc. Jpn.*, 1966, **39**, 369.
- 41 Z. Galus, *Fundamentals of Electrochemical Analysis*, Ellis Harwood, Chichester, 1976. See also Howell *et al.* in ref. 32.
- 42 C. S. Yang, Y. Y. Wang and C. C. Wan, *J. Electrochem. Soc.*, 1989, **136**, 2592.
- 43 *Molecular Complexes*, ed. R. Foster, Crane, Russak, New York, (a) R. Foster, vol. 2, 1974, p. 107 ff; (b) M. W. Hanna and J. L. Lippert, vol. 1, 1973, p. 1 ff.
- 44 V. E. Kampar and O. Ya. Neiland, *Zhur. Obsh. Khim.*, 1977, **47**, 442.
- 45 A. Bard and L. Faulkner, *Electrochemical Methods*, Wiley, New York, 1980.
- 46 Compare: R. J. Klingler and J. K. Kochi, *J. Am. Chem. Soc.*, 1980, **102**, 4790.
- 47 T. Umemoto, S. Fukami, G. Tomizawa, K. Harasawa, K. Kawada and K. Tomita, *J. Am. Chem. Soc.*, 1990, **112**, 8563.
- 48 T. Sumiyoshi, M. Katayama and W. Schnabel, *Bull. Chem. Soc. Jpn.*, 1988, **61**, 1893; R. Fielden and L. A. Summers, *J. Heterocycl. Chem.*, 1974, **44**, 299.
- 49 See: D. J. Kuchynka and J. K. Kochi, *Inorg. Chem.*, 1989, **28**, 855.
- 50 A. Bard and L. Faulkner in ref. 45, p. 488 ff.

Paper 2/01334G

Received 12th March 1992

Accepted 3rd April 1992